

Rheology-Processing-Property Relationships in Tubular Blown Film Extrusion. II. Low-Pressure Low-Density Polyethylene

TAE HOON KWACK and CHANG DAE HAN, *Department of Chemical Engineering, Polytechnic Institute of New York, Brooklyn, New York 11201*

Synopsis

An experimental investigation was undertaken to establish rheology-processing-property relationships in the tubular blown film extrusion of low-pressure low-density polyethylene (LP-LDPE). For the study, three commercial LP-LDPE resins, each from a different resin manufacturer, were used in producing tubular films, by employing the apparatus described in Paper I of this series. Both molecular and rheological characterizations of the resins were conducted, enabling us to interpret the tubular film blowing characteristics of the resins. Correlations were obtained between the processing variables (namely, blowup and takeup ratios) and the tensile properties of the films. The tubular film blowing characteristics of LP-LDPE and HP-LDPE resins are compared. Differences in the rheological properties (namely, elongational viscosity) of the two types of resin are used in explaining the experimentally observed differences in their tubular film blowability.

INTRODUCTION

Recent developments in manufacturing low-density polyethylene resins at low pressures, by means of either liquid phase or gas phase polymerization, have stimulated the interest of the film-producing industry.^{1,2} It is reported that films produced from low-pressure low-density polyethylene (LP-LDPE) resins have mechanical and optical properties superior to those produced from high-pressure low-density polyethylene (HP-LDPE) resins.^{3,4}

One interesting aspect of LP-LDPE resins is that they contain little or no long-chain branching (LCB) and attain their low densities (ca. 0.92 g/cm³) by virtue of copolymerization of ethylene with α -olefins such as butene-1, hexene-1, or octene-1. In their recent study, Wild et al.⁵ reported that LP-LDPE resins have substantial amounts of short-chain branching (SCB). For the study, they employed a temperature-rising elution fractionation technique.⁶

It is also reported⁴ that LP-LDPE resins have relatively narrow molecular weight distributions (MWD) compared to those of HP-LDPE. It may be surmised that a change in molecular structure brings about different rheological responses, thus requiring different processing conditions and consequently resulting in different physical, mechanical, or optical properties in the fabricated products. It has been claimed,⁴ for instance, that LP-LDPE films have higher tensile strength and elongation, outstanding film puncture resistance, greater stiffness, excellent environmental stress crack resistance, and outstanding draw-down characteristics, compared to HP-LDPE films.

However, only a few fundamental studies^{3,4} have been published that discuss the processing characteristics of LP-LDPE resins and their ultimate mechanical

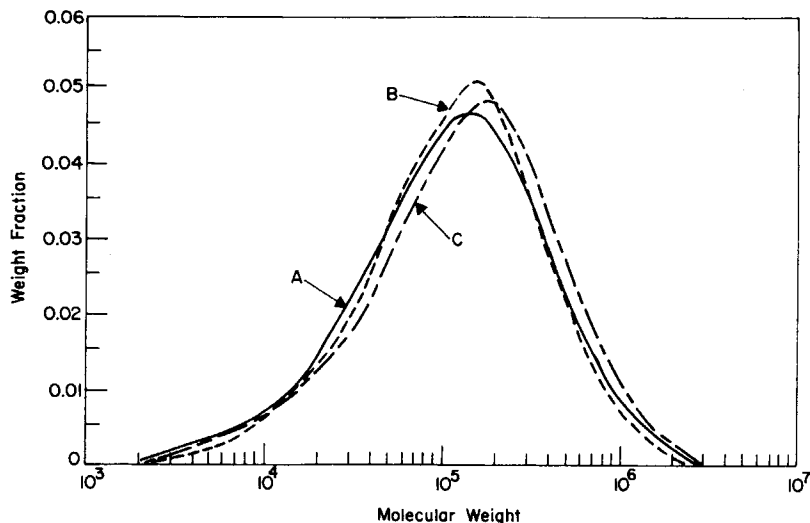


Fig. 1. Molecular weight distribution curves for the three low-pressure low-density polyethylenes (LP-LDPE) investigated.

properties. As part of our continuing effort on enhancing our understanding of tubular blown film extrusion, we have very recently conducted a study of the process, using three different grades of LP-LDPE resin. In this paper, we shall present the highlights of our results.

EXPERIMENTAL

The materials used were three LP-LDPE resins, each produced by a different resin manufacturer. Figure 1 gives the molecular weight distribution curves of the three resins, and Table I gives their molecular weights (number average molecular weight \bar{M}_n and weight average molecular weight \bar{M}_w). We understand that resin A and resin B were produced by solution polymerization and that they are copolymers of ethylene and α -olefins, such as hexene or octene. On the other hand, resin C was produced by a gas-phase polymerization process, and it is a copolymer of ethylene and C_3 - C_6 α -olefins.¹

The shear flow properties are given in Figure 2, and the elongational viscosities are given in Figure 3, for the three LP-LDPE resins investigated. The experimental techniques employed are the same as those described in Paper I of this series.⁷

The tubular film blowing experiment was conducted, using the apparatus

TABLE I
Molecular Characteristics of the LP-LDPE Resins Employed

Resin manufacturer	Sample code	\bar{M}_n	\bar{M}_w	\bar{M}_w/\bar{M}_n	ρ (g/cm ³)	Melt index
Dow Chemical	A	5.72×10^4	2.51×10^5	4.40	0.920	1.00
Mitsui Petrochemical	B	5.60×10^4	2.21×10^5	3.95	0.921	2.00
Union Carbide	C	7.60×10^4	2.80×10^5	3.70	0.919	0.86

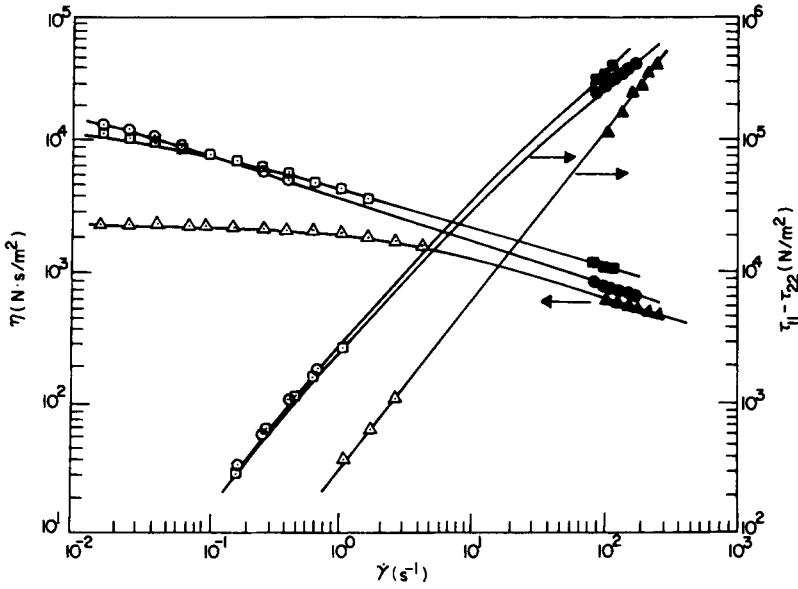


Fig. 2. η and $\tau_{11} - \tau_{22}$ vs. $\dot{\gamma}$ at 240°C for: (○, ●) resin A; (△, ▲) resin B; (□, ■) resin C; (○, △, □) data taken with a cone-and-phase rheometer, (●, ▲, ■) data taken with a slit/capillary rheometer.

described in Paper I of this series.⁷ The details of the experimental procedure employed are also described in the same paper.

RESULTS AND DISCUSSION

Tubular Film Blowing Characteristics

Figure 4 gives plots of S_{11F} and S_{33F} vs. blowup ratio (BUR) for resin A, with takeup ratio (TUR) as parameter. Similar plots are given in Figure 5 for resin

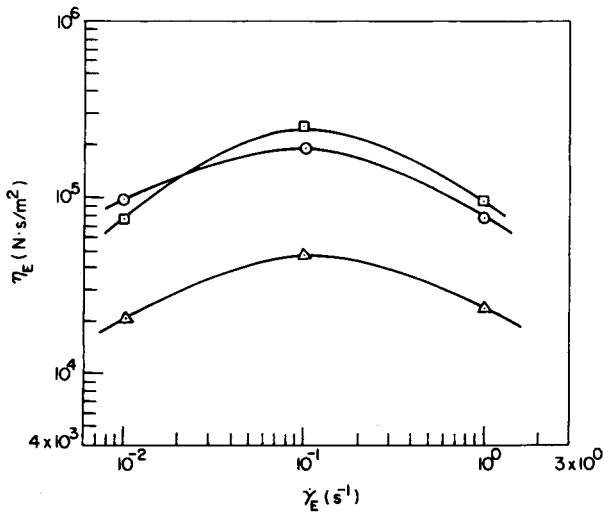


Fig. 3. η_E vs. $\dot{\gamma}_E$ at 180°C for: (○) resin A; (△) resin B; (□) resin C.

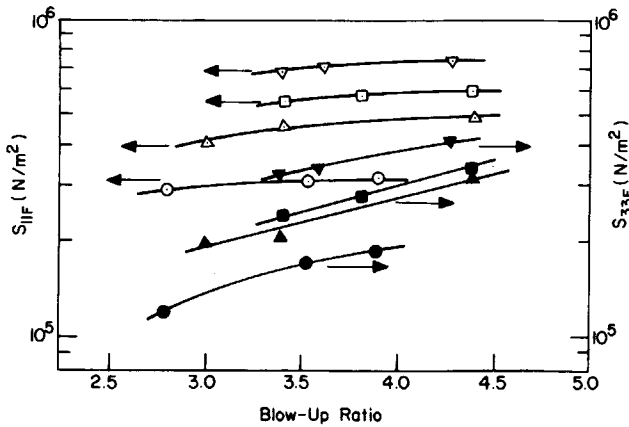


Fig. 4. S_{11F} and S_{33F} vs. blowup ratio for resin A at various take-up ratios: (○, ●) 7.6; (△, ▲) 11.0; (□, ■) 14.3; (▽, ▼) 17.4. Other processing conditions are: Melt temperature 220°C; Cooling air flow rate 2883 cm³/s.

B and in Figure 6 for resin C. Note in these figures that S_{11F} and S_{33F} are the tensile stresses in the machine and transverse direction, respectively, at the freeze line, and they were calculated by the use of eqs. (8) and (9) in Paper I of this series.⁷ Figures 7–9 describe the effect of cooling air flow rate on the S_{11F} and S_{33F} of the three LP-LDPE's investigated. A close examination of Figures 4–6 reveals, however, that the three resins give rise to, under identical processing conditions, different values of S_{11F} and S_{33F} . This is attributable to the subtle difference existing in their molecular characteristics (see Table I). The same observation can be made on Figures 7–9. Note in Figures 7–9 that an increase in cooling air flow rate (i.e., a faster cooling of the tubular bubble, upon exiting the die) increases the values of S_{11F} and S_{33F} . It should be pointed out that faster cooling decreases the freeze-line height, and undoubtedly influences the crystalline orientation and morphology, and hence the mechanical/optical properties, of the film produced.

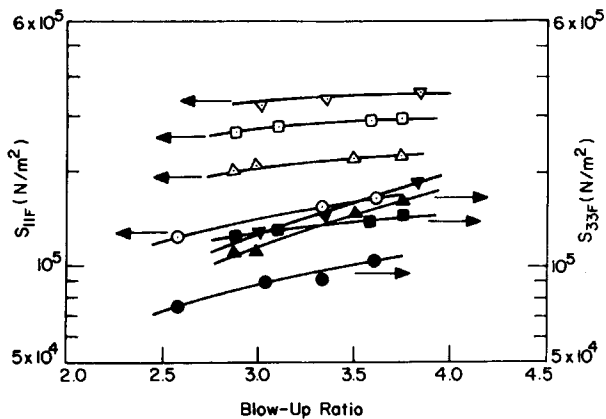


Fig. 5. S_{11F} and S_{33F} vs. blowup ratio for resin B at various take-up ratios. Symbols and other processing conditions are the same as in Figure 4.

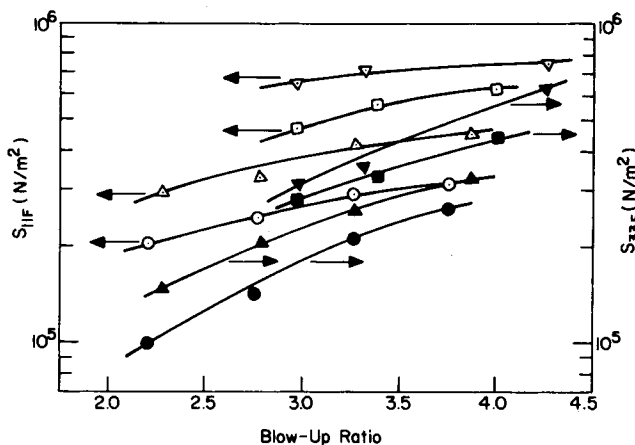


Fig. 6. S_{11F} and S_{33F} vs. blowup ratio for resin C at various takeup ratios. Symbols and other processing conditions are the same as in Figure 4.

It is seen in Figures 4–9 that, as the BUR is increased, any increase in S_{11F} is hardly perceptible and the increase in S_{33F} is rather slow. It is of interest to note that the increase in S_{33F} with BUR for the LP-LDPE's is very small, compared to that for the HP-LDPE's reported in Paper I of this series.⁷ In view of the fact that an increase in BUR increases the rate of strain, qualitatively speaking, the shape of the curves given in Figures 4–9 describes the elongational behavior of the material at the freeze line, *albeit* a quantitative interpretation is very difficult to make because of the effect of cooling. With this understanding, one may surmise from Figures 4–9 that the elongational viscosity would exhibit a decreasing trend with increasing elongation rate (i.e., extensional-thinning behavior), because the tensile stresses (S_{11F} and S_{33F}) increase very slowly as the elongation rate (via BUR) is increased.

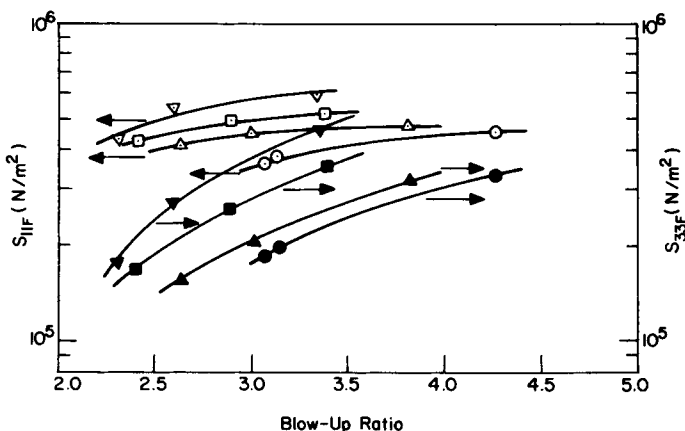


Fig. 7. S_{11F} and S_{33F} vs. blowup ratio for resin A at various values of cooling air flow rate (cm^3/s): (\circ , \bullet) 2567; (\triangle , \blacktriangle) 2883; (\square , \blacksquare) 3200; (∇ , \blacktriangledown) 3510. Other processing conditions are: takeup ratio 11.0; melt temperature 220°C .

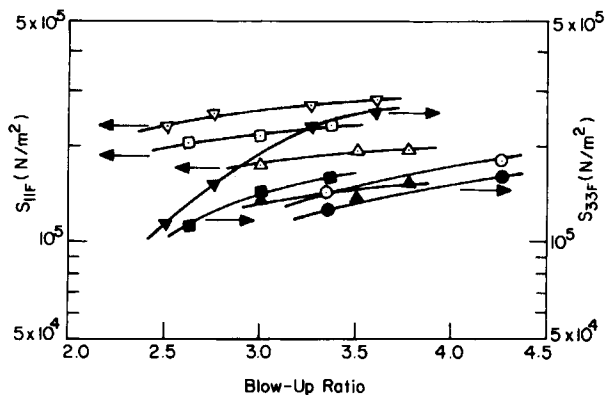


Fig. 8. S_{11F} and S_{33F} vs. blowup ratio for resin B at various values of cooling air flow rate. Symbols and other processing conditions are the same as in Figure 7.

Figure 10 gives plots of S_{11F} and S_{33F} vs. BUR at a fixed value of TUR, and Figure 11 gives plots of S_{11F} and S_{33F} vs. TUR at a fixed value of BUR, for the three resins employed. It is seen that, at constant values of TUR and BUR, resin B has the lowest value of S_{11F} and S_{33F} , suggesting that it has the lowest value of elongational viscosity of the three resins employed. This observation, though qualitative, is borne out by the independently performed elongational flow experiment that is summarized in Figure 3.

Figure 12 gives plots of tensile stress S_{11} vs. time for the three LP-LDPE resins employed, when subjected to a uniaxial elongational flow. Since the experiment was performed at constant values of elongation rate, the elongational viscosity η_E may be plotted against time, with elongation rate as parameter, as shown in Figure 13. It is of interest to note that steady state is attained by each resin at three different elongation rates, and that the values of η_E at $\dot{\gamma}_E = 1.0 \text{ s}^{-1}$ are smaller than those at $\dot{\gamma}_E = 0.1 \text{ s}^{-1}$ for all three. (See the plots of η_E vs. $\dot{\gamma}_E$ given in Figure 3.)

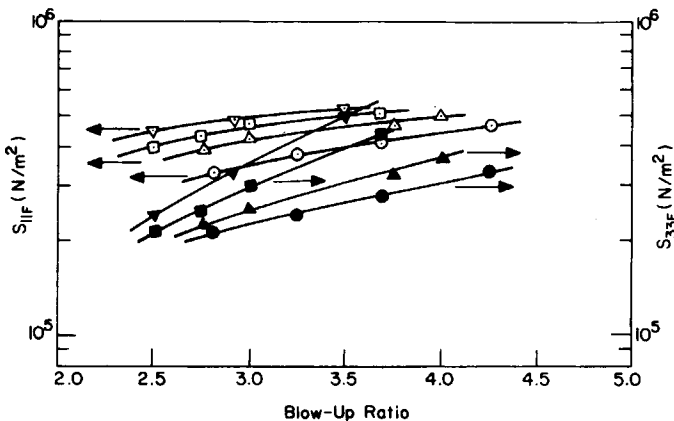


Fig. 9. S_{11F} and S_{33F} vs. blowup ratio for resin C at various values of cooling air flow rate. Symbols and other processing conditions are the same as in Figure 7.

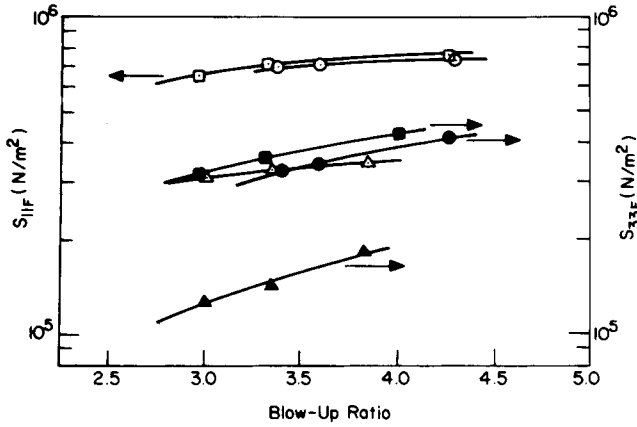


Fig. 10. S_{11F} and S_{33F} vs. blowup ratio at a takeup ratio of 17.5, for three LP-LDPE's: (○, ●) resin A; (△, ▲) resin B; (□, ■) resin C. Other processing conditions: melt temperature 220°C; cooling air flow rate 2883 cm³/s.

During the tubular film blowing experiment, at several fixed blowup ratios, we increased the takeup speed stepwise in order to break the tubular film. However, within the limit of our equipment (capable of a maximum TUR of about 80) we could *not* break the tubular film. In other words, as we increased the speed of the takeup roll to its limiting value, the tubular film was stretched continuously without having cohesive failure. It should be remembered that, in extruding HP-LDPE, we were able to break the tubular film at a maximum TUR below 60, as summarized in Figure 12 in Paper I of this series.⁷ In other words, due to the excellent drawability of the LP-LDPE's employed, the tensile force applied could not bring about the cohesive failure of the tubular bubble, under the processing conditions chosen in our experiment.

As either the takeup speed or the blowup ratio is increased during a tubular film blowing operation, the tubular bubble will eventually break when the tensile stress exerted exceeds a critical value that the tubular bubble can no longer

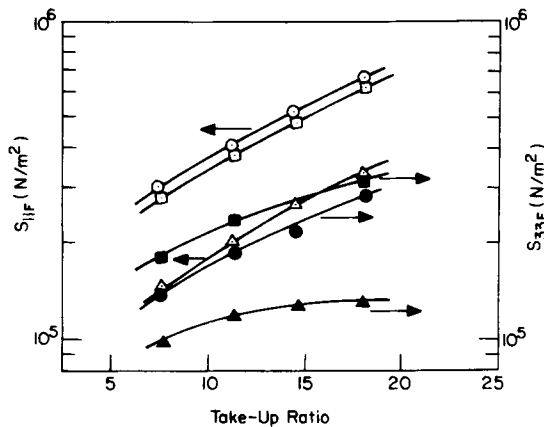


Fig. 11. S_{11F} and S_{33F} vs. takeup ratio at a blowup ratio of 3.0, for three LP-LDPE's. Symbols and other processing conditions are the same as in Figure 10.

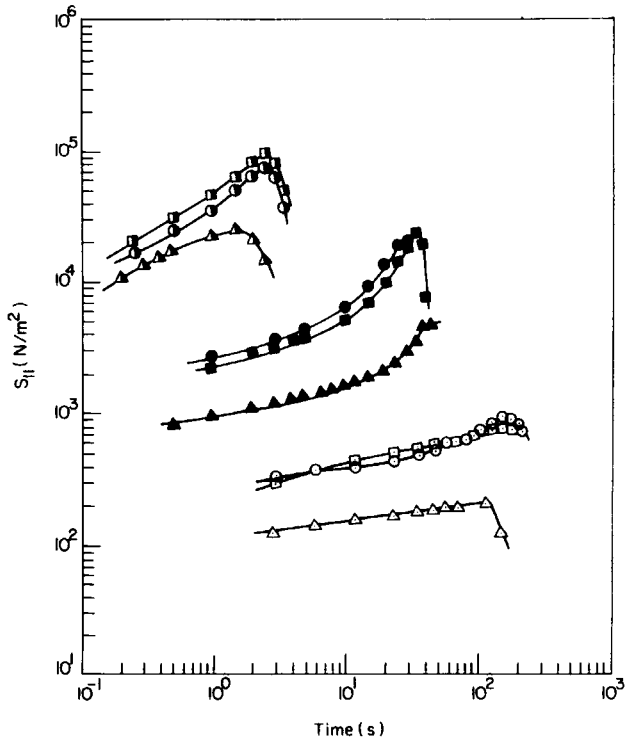


Fig. 12. Tensile stress vs. time in uniaxial elongational flow at 180°C. (a) Resin A at various values of constant elongation rate (s^{-1}): (\odot) 0.01; (\bullet) 0.10; (\ominus) 1.00. (b) Resin B at various values of constant elongation rate (s^{-1}): (\triangle) 0.01; (\blacktriangle) 0.10; (\blacktriangle) 1.00. (c) Resin C at various values of constant elongation rate (s^{-1}): (\square) 0.01; (\blacksquare) 0.10; (\blacksquare) 1.00.

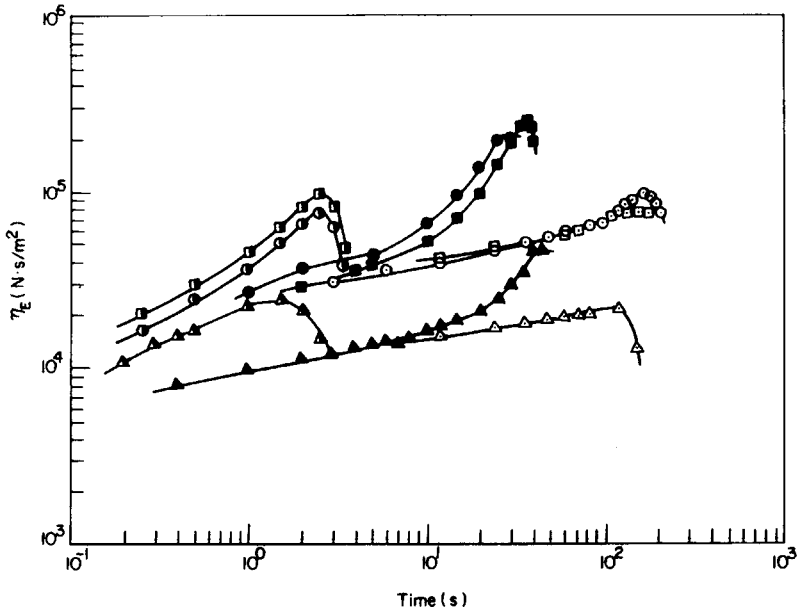


Fig. 13. Elongational viscosity versus time in uniaxial elongational flow at 180°C. Symbols are the same as in Figure 12.

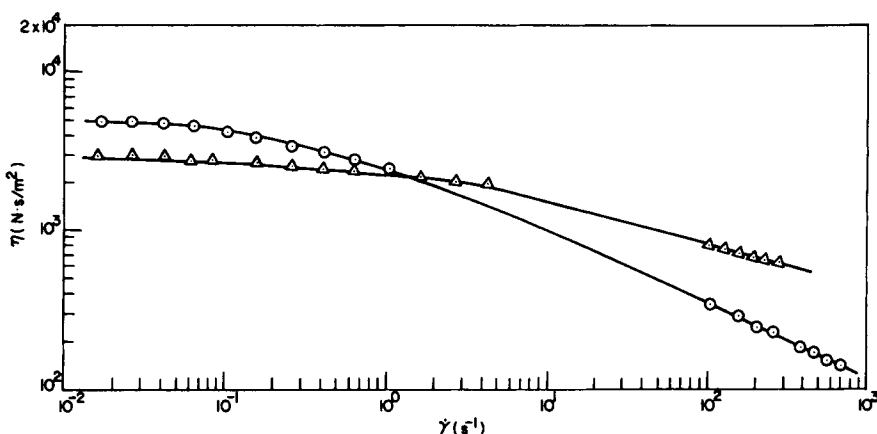


Fig. 14. η vs. $\dot{\gamma}$ at 220°C for: (○) HP-LDPE (Dow PE 510); (△) LP-LDPE (resin B).

withstand. Such a critical stress, that may be termed *ultimate* melt strength, must be inherent in the molecular parameters of a given polymer and in its molecular structure. Note that, as the takeup speed and/or the blowup ratio is increased, the tubular film will be stretched, giving rise to thinner films. If a polymer melt exhibits *strain-hardening* behavior, the tensile stress of the melt will increase very rapidly and thus will reach the critical value (i.e., ultimate melt strength) before the film can be stretched further. On the other hand, if a polymer melt exhibits *strain-softening* behavior, the tensile stress of the melt will increase rather slowly and thus the tubular film will be stretched greatly before the tensile stress in the melt reaches its critical value. In other words, the stretching operation will cause the stress to build up much faster in an HP-LDPE melt than in an LP-LDPE melt, thus reaching the critical value of melt strength at a strain rate much lower with HP-LDPE than with LP-LDPE. Therefore, one can conclude that LP-LDPE permits greater draw-down ratios (hence thinner films) than HP-LDPE does.

At this juncture it is worth elaborating on the shear-thinning behavior of the LP-LDPE's employed. In order to facilitate our discussion here, let us refer to Figure 14, in which the LP-LDPE-B (see Table I above) is compared with a typical HP-LDPE (Dow PE 510). The power-law index n for the LP-LDPE-B is 0.62, whereas the value for the HP-LDPE is 0.45. Note that the LP-LDPE-B has values of $\bar{M}_n = 5.60 \times 10^4$ and $\bar{M}_w = 2.21 \times 10^5$, which are greater than those for the HP-LDPE ($\bar{M}_n = 1.39 \times 10^4$ and $\bar{M}_w = 1.12 \times 10^5$). Note also that both resins have identical melt indexes ($MI = 2.0$). The fact that the HP-LDPE has a larger value of zero-shear viscosity (η_0) than the LP-LDPE-B, in spite of the fact that the former has smaller values of \bar{M}_n and \bar{M}_w than the latter, may be attributable to the greater amount of entanglement caused by the presence of long-chain branching (LCB) in the HP-LDPE. In other words, the amount of energy required for disentangling the large molecules of branched HP-LDPE, when they are virtually at the state of rest, is greater than that for LP-LDPE-B that contains little or no LCB and only short-chain branching (SCB). Once the macromolecules are sufficiently disentangled under shearing motion (i.e., at and above a critical value of shear rate), the number average molecular weight (\bar{M}_n)

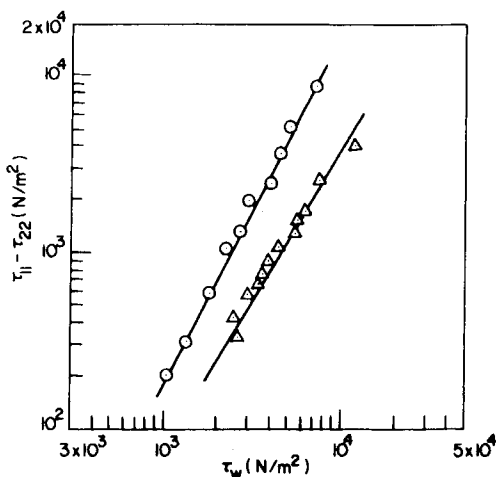


Fig. 15. $\tau_{11} - \tau_{22}$ versus τ_w at 220°C for: (○) HP-LDPE (Dow PE 510); (△) LP-LDPE (resin B).

may be the controlling factor in determining the amount of energy required for shearing the macromolecules.

At this juncture, it is worth pointing out that the melt index (MI), widely used in marketing thermoplastic resins, has *little* rheological significance. As may be seen in Figure 14, the two resins have an identical viscosity at one shear rate ($\dot{\gamma} = 1.5 \text{ s}^{-1}$), i.e., $MI = 2.0$ indicates a single value of viscosity at the particular flow condition (i.e., shear rate) chosen. On the other hand, the shear rates encountered in practical extrusion operations are somewhere between 500–2000 s^{-1} . Therefore, knowing the value of MI provides no help in predicting what the viscosities of a resin will be at high shear rates of practical interest.

Figure 15 gives a comparison of the first normal stress differences of the LP-LDPE-B and the HP-LDPE. It is seen that the HP-LDPE is much more elastic than the LP-LDPE-B. This is attributable to the presence of long-chain branching.

Tensile Properties of the Tubular Blown Films

Figure 16 gives the effect of TUR, and Figure 17 gives the effect of BUR, on the tensile strength (which is the engineering stress developed at break) in both the machine direction (MD) and transverse direction (TD), of LP-LDPE-B tubular blown films extruded at two different melt temperatures. It is seen that the tensile strengths in both MD and TD are greater when the films are extruded at 200°C, than when extruded at 220°C. This observation is consistent with our intuitive expectation that films produced in a cold drawing operation have mechanical properties superior to those obtained in a melt drawing operation. Note that the magnitude of the stress imposed on the tubular bubble is greater when it is extruded at 200°C, than extruded at 220°C.

Figure 18 gives plots of MD and TD tensile strengths vs. BUR for the three LP-LDPE's investigated. It is seen that, under a certain combination of BUR and TUR, the MD tensile strength becomes identical to the TD one.

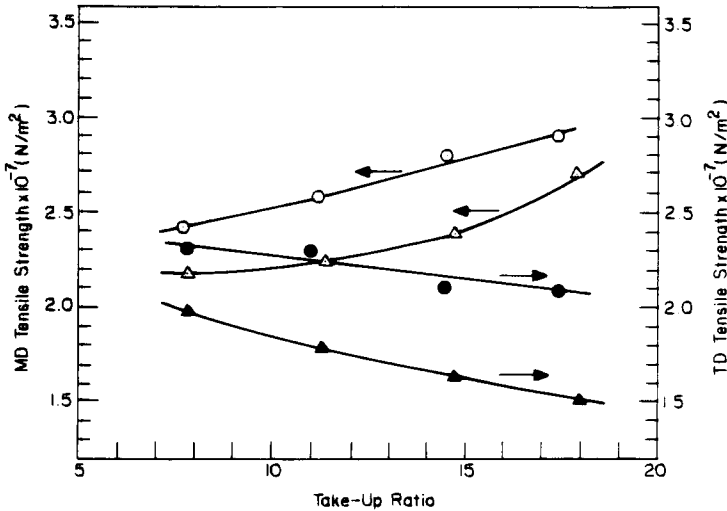


Fig. 16. Machine direction (MD) and transverse direction (TD) tensile stresses vs. take-up ratio for resin B at two different melt temperatures (°C): (○, ●) 200; (△, ▲) 220. Other processing conditions are: blowup ratio 3.0; cooling air flow rate 2883 cm³/s.

Figure 19 gives plots of S_{11F}/S_{33F} ratio vs. BUR for the three LP-LDPE resins. For comparison purposes, similar plots are also given for the HP-LDPE resins investigated in Paper I of this series.⁷ It is seen clearly that, under comparable processing conditions, a more uniform tensile strength in the MD and TD is achievable with LP-LDPE resins than with HP-LDPE resins. This may be attributable to the absence of long side chain branching in LP-LDPE resins. Crystallization takes place at the freeze line, i.e., at the position in the machine direction where the tubular bubble begins to solidify and forms a constant bubble diameter. It also takes place under biaxial stretching. Therefore, in order to understand how the ultimate mechanical properties of LP-LDPE are obtained,

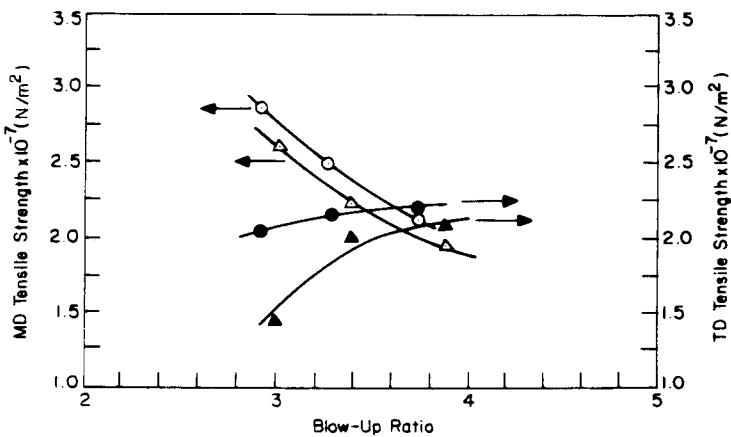


Fig. 17. MD and TD tensile stresses vs. blowup ratio for resin B at two different melt temperatures (°C): (○, ●) 200; (△, ▲) 220. Other processing conditions are: takeup ratio 18.0; cooling air flow rate 2883 cm³/s.

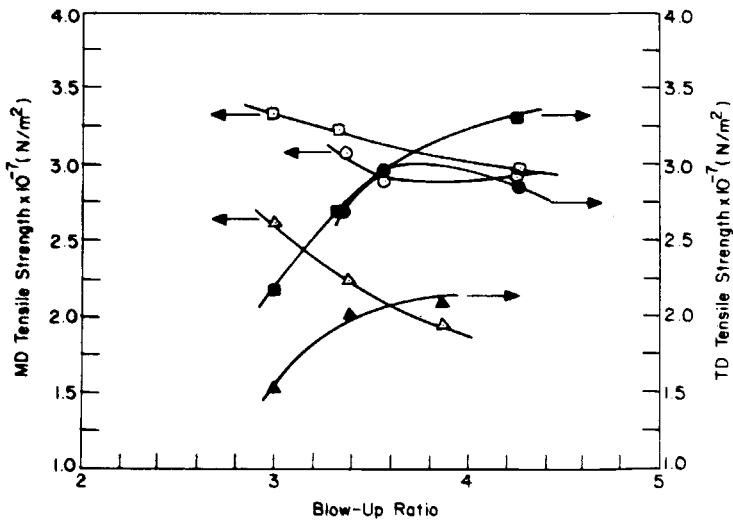


Fig. 18. MD and TD tensile stresses vs. blowup ratio for three LP-LDPE's: (○, ●) resin A; (△, ▲) resin B; (□, ■) resin C. Other processing conditions are: takeup ratio 18.0; melt temperature 220°C; cooling air flow rate 2883 cm²/s.

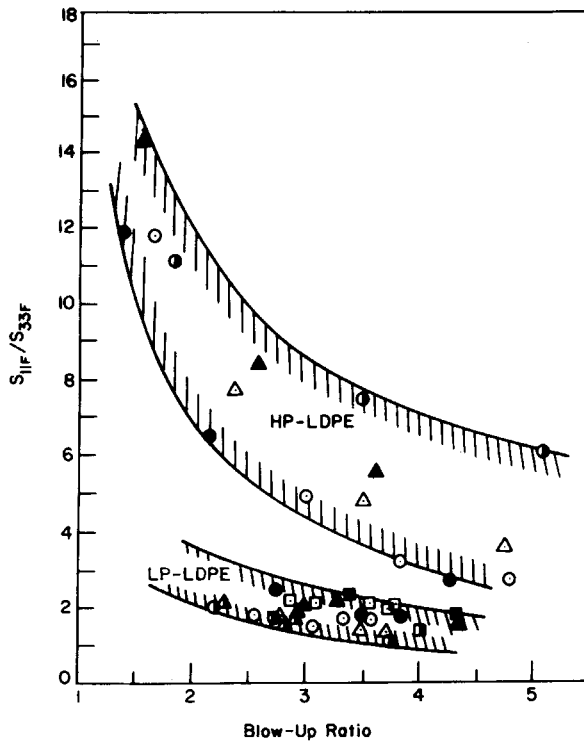


Fig. 19. S_{11F}/S_{33F} ratio vs. blowup ratio for three LP-LDPE's. (a) Resin A at various takeup ratios: (●) 7.6; (▲) 11.0; (■) 14.3. (b) Resin B at various takeup ratios: (○) 7.6; (△) 11.0; (□) 14.3. (c) Resin C at various takeup ratios: (○) 7.6; (▲) 11.0; (■) 14.3.

TABLE II
Optical Properties of the LP-LDPE Blown Film Samples^a

Resin	BUR	TUR	45° specular gloss	Haze (%)
A	3.0	11.0	37.9	15.8
B	2.9	11.0	59.7	9.5
C	2.8	11.0	39.7	14.6

^a Melt extrusion temp 220°C; cooling air flow rate 2883 cm³/s.

we must consider many structural factors. These include the presence of short-chain branching, the amorphous orientation function, the degree of crystallinity, the distribution of crystalline axis orientation, and the morphological structure. Note that these structural factors are strongly influenced by processing conditions in a very complicated manner. Further research in this area is urgently needed.

Optical Properties of the Tubular Blown Films

Table II gives a summary of typical optical properties (namely, 45° specular gloss and haze) of the LP-LDPE tubular blown films. It is seen that, of the three resins employed, resin B has the highest value of gloss and the lowest value of haze. Note that the optical properties are strongly related to the size of crystalline domain, which in turn is strongly influenced by the processing conditions, particularly by the rate of cooling.

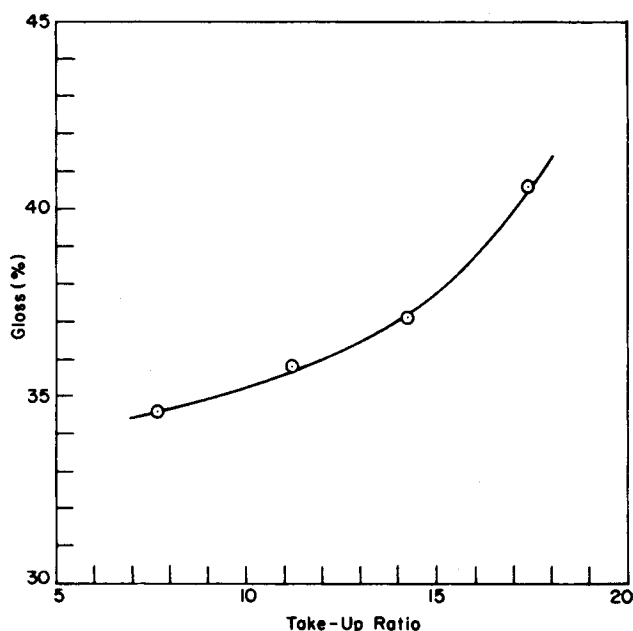


Fig. 20. Gloss vs. take-up ratio for resin A. Processing conditions are: melt temperature 220°C; blowup ratio 3.4; cooling air flow rate 2883 cm³/s.

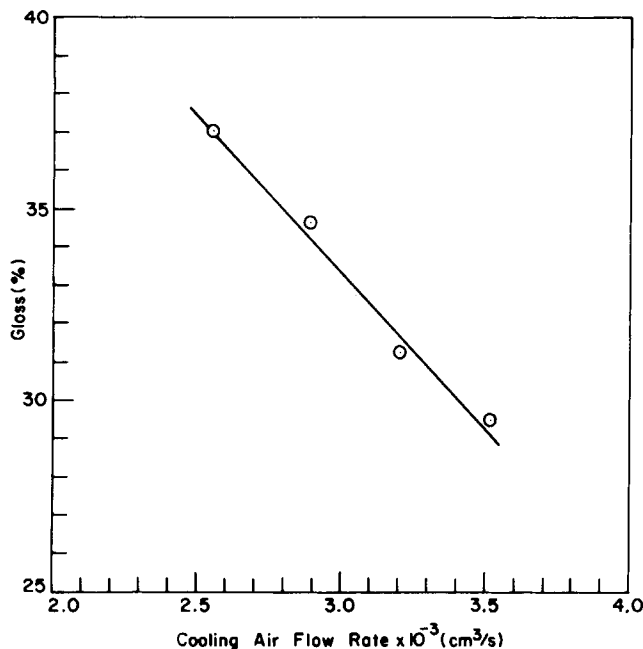


Fig. 21. Gloss vs. cooling air flow rate for resin A. Processing conditions are: melt temperature 220°C; blowup ratio 3.2; takeup ratio 11.0.

Figure 20 describes the effect of takeup ratio (TUR), and Figure 21 the effect of cooling air flow rate, on the gloss of the tubular film produced from resin A. It is seen that the gloss of the film was increased as the TUR was increased and, also, as the tubular bubble was cooled slowly. Note that the tubular bubble is cooled slowly as the TUR is increased. Therefore, we can conclude from Figures 20 and 21 that the gloss of the film is strongly influenced by the rate of cooling of the tubular bubble, upon exiting from the die. Frazer and Cieloszyk⁴ have reported an empirical correlation that relates the gloss of the tubular film produced to the processing conditions.

A general trend is seen in Table II above, when compared with Table II in Paper I of this series,⁷ that the haze of LP-LDPE is greater than that of HP-LDPE. Note that the haze (or gloss) of tubular blown films depends on the extent of the surface irregularities and the size of crystalline domain in the films, which in turn are influenced by the processing conditions. At present, we are not certain about how much of the observed differences in haze is attributable to the structural difference between the two types of the LDPE resin investigated. This subject is certainly worth investigating in the future.

CONCLUDING REMARKS

It has been demonstrated that the rheological behavior of LP-LDPE resin is quite different from that of HP-LDPE resin, namely: (1) the LP-LDPE is less shear thinning than the HP-LDPE; (2) for a given shear stress, the normal stress difference $\tau_{11} - \tau_{22}$ of the LP-LDPE is smaller than that of the HP-LDPE; (3) the elongational viscosity η_E of the LP-LDPE initially increases and then de-

creases as the elongation rate $\dot{\gamma}_E$ increases from 0.01 to 1.0 s⁻¹, whereas the η_E of the HP-LDPE increases with $\dot{\gamma}_E$ over the same range. The excellent tubular film blowability of LP-LDPE, observed experimentally, is attributable to the decreasing trend of η_E with increasing $\dot{\gamma}_E$, at high elongation rates. We have found that we could achieve an equality of tensile properties in the MD and TD (i.e., films having $S_{11F}/S_{33F} = 1$), because of the greater drawability of LP-LDPE resins.

In future, our efforts will be applied to investigating the mechanism of crystalline orientation and the development of the morphology of the crystalline phase, as affected by the presence of short-chain branching and by the processing conditions.

We wish to acknowledge that Mr. Yong Joo Kim measured high-shear flow properties, and Mr. Hsiao-Ken Chuang the low-shear flow properties, of the resins investigated, and that Professor James L. White at the University of Tennessee allowed us to use the elongational rheometer in his laboratory.

References

1. I. J. Levine and F. J. Karol, U.S. Pat. 4,011,382 (1977).
2. Y. Morita and H. Inoue, U.S. Pat. 4,205,021 (1980).
3. W. A. Fraser, L. S. Scarola, and M. Concha, TAPPI Paper Synthetics Course Processings, Technical Association of the Pulp and Paper Industry, Inc., Atlanta, Ga., 1980, p. 237.
4. W. A. Fraser and G. S. Cieloszyk, U.S. Pat. 4,243,619 (1981).
5. L. Wild, T. Ryle, and D. Knobloch, *Am. Chem. Soc., Polym. Prepr.*, **47**, 133 (1982).
6. L. Wild, T. Ryle, D. C. Knobloch, and I. R. Peat, *J. Polym. Sci., Polym. Phys. Ed.*, **20**, 441 (1982).
7. C. D. Han and T. H. Kwack, *J. Appl. Polym. Sci.*, **28**, 3399 (1983).

Received November 9, 1982

Accepted May 20, 1983